Int. J. Heat Mass Transfer. Vol. 11, pp. 1253–1265. Pergamon Press 1968. Printed in Great Britain

TRANSIENT RESPONSE OF COUNTERCURRENT HEAT EXCHANGERS WITH SHORT CONTACT TIME

P. F. TOMLAN and J. L. HUDSON

Department of Chemistry and Chemical Engineering, University of Illinois, Urbana, Illinois, U.S.A.

(*Received* 3 *July* 1967 *and in revised form* 26 *February* 1968)

Abstract—Numerical solutions are obtained for steady-state and transient behavior in countercurrent heat exchangers with short contact time. For the steady-state solution, two simplified velocity profiles are used: plug flow and a linear velocity profile. The results are compared to the classical solution of using addition of resistances, where either the wall temperature or the wall heat flux is assumed to be constant.

The transient problem resulting from a flow rate change in one of the streams is solved assuming plug flow and a series approximation for the wall temperature. This is compared to a simplified model using an average wall temperature independent of position but varying with time. Overshoots in the average wall flux are found to occur in both models when the ratio of the velocity of the perturbed stream to the velocity of the other stream is greater than one.

NOMENCLATURE

A, $= \dfrac{\rho_1 C_{p_1} u_1 k_2}{\rho_2 C_{p_2} u_2 k_1}$, for plug flow;

$= \dfrac{\rho_1 C_{p_1} S_1 k_2}{\rho_2 C_{p_2} S_2 k_1}$, for linear velocity profiles;

B, $= u_1/u_2$, for plug flow;

B, $= S_1/S_2$, for linear velocity;

C_p, heat capacity;

h_1, heat-transfer coefficient for stream one, $= q/(T_w - T_i)$;

h_2, heat-transfer coefficient for stream two, $= q/(T_L - T_w)$;

k, thermal conductivity;

L, length of heat exchanger;

p, Laplace transform variable related to τ;

q, heat flux at wall, $= -k\partial T/\partial y|_{y=0}$;

Q, dimensionless heat flux at wall, $= -\partial\theta/\partial\eta|_{\eta=0}$;

Q_t, perturbation of heat flux from steady state, $= -\partial\theta_{1t}/\partial\eta|_{\eta=0}$;

s, Laplace transform variable related to ξ;

S, slope of velocity at the wall, $= \partial u/\partial y|_{y=0}$;

t, time;

T, temperature;

T_t, perturbation of temperature from steady state;

u, velocity;

U, overall heat-transfer coefficient;

W, expansion function in equation (23);

x, axial distance;

y, distance from wall.

Greek symbols

β, $= \left(\dfrac{\rho_1 C_{p_1} u_1 k_1}{\rho_2 C_{p_2} u_2 k_2}\right)^{\frac{1}{2}}$;

γ, $= \left(\dfrac{\rho_1 C_{p_1} S_1 k_1^2}{\rho_2 C_{p_2} S_2 k_2^2}\right)^{\frac{1}{3}}$;

η, $= \left(\dfrac{\rho_1 C_{p_1} u_1}{k_1 L}\right)^{\frac{1}{2}} y$, for plug flow;

η, $= \left(\dfrac{\rho_1 C_{p_1} S_1}{k_1 L}\right)^{\frac{1}{3}} y$, for linear velocity profile;

θ, $= (T - T_i)/(T_L - T_i)$;

θ_t, $= T_t/(T_L - T_i)$;

ξ, $= x/L$;

ρ, fluid density;

τ, tu_1/L;

ψ, time dependence in transient temperature expansion.

Subscripts

0, initial conditions;

1, stream one;
2, stream two;
i, inlet condition of stream one;
L, inlet condition of stream two;
t, transient dependence;
T, constant wall temperature;
Q, constant wall heat flux;
w, wall conditions.

Superscripts

$-$, average value over length of heat exchanger;
$\hat{}$, Laplace transform.

INTRODUCTION

IN THE design or analysis of cocurrent or countercurrent heat exchangers the overall heat-transfer coefficient U is usually used where U is defined by

$$\frac{1}{U} = \frac{1}{h_1} + \frac{1}{h_2}. \tag{1}$$

The individual heat-transfer coefficients h_1 and h_2 are assumed to be independent of each other; each of the coefficients h_1 and h_2 is assumed to be that which would arise with a known wall temperature or heat flux in the absence of the other stream.

A more exact method of analysing heat exchangers with countercurrent or cocurrent flow is to simultaneously solve the governing energy equations for the two streams. The heat flux between the fluids is equated at each point along the surface. The temperatures of the two streams are also related at the surface and are equal if the resistance of the surface is neglected. Several analyses of steady-state heat transfer have been made using this approach. Nunge and Gill [1, 2] and Stein [3–5] have recently considered heat transfer between fully-developed countercurrent flows. Solutions were obtained in terms of a series of orthogonal functions; the solutions are interesting extensions of the Graetz problem. A detailed discussion of the mathematics used in analyses of cocurrent and countercurrent flow heat transfer is presented by Blanco and Gill [6]; extensions are also made to the multistream problem and to turbulent flow. Axial conduction in the fluid streams is considered by Nunge, Porta and Gill [7]. Countercurrent flow with a short contact time of a laminar and turbulent stream has been considered by Lightfoot [8]. A constant local heat-transfer coefficient was used for the turbulent fluid. King [9] has treated transport in laminar countercurrent flow with short contact time. Two models were used: one stream was in plug flow and the second in plug flow or having laminar boundary-layer behavior. The heat flux between the two streams is greater than that obtained from equation (1) where h_1 and h_2 are based on a uniform temperature wall. Transport between two cocurrent streams has also been considered by Stein [3, 10, 11] with the use of an orthogonal series expansion.

The rate of transport between countercurrent or cocurrent streams and the errors which would arise from the use of equation (1) can thus be predicted in certain steady-state situations. Consideration is given here to the transient case for which previous studies have been made using equation (1), e.g. [12, 13]. The velocity of one of the streams will undergo a step change and the response of the system determined. The energy equations for the two streams, along with the boundary conditions equating the wall temperatures and heat fluxes of the two streams, are solved. The results will then be compared to a simpler model which assumes that the wall temperature is independent of position. This comparison is analogous to the comparison of the calculated steady-state solution with the steady-state solution found by assuming a constant wall temperature, i.e. by employing equation (1). In order to simplify the computation, a plug flow velocity profile is assumed for both streams. It is further assumed that the contact time is short so that temperature changes propagate only a short distance into either stream so that boundary conditions at infinity may be employed. Since the plug flow model is used in the transient analysis, it was

desired to first make further comparisons of the steady-state results using a plug flow model to results found by employing a more realistic velocity profile. Steady-state calculations are therefore made using a linear velocity profile for each fluid. The heat flux predicted by the linear velocity profile model lies between that predicted from the plug flow model and that predicted from the use of an overall heat-transfer coefficient from equation (1). King's results [9] obtained for a plug flow in one stream and boundary-layer behavior in the second stream also lie between the results for plug flow and from the use of an overall heat-transfer coefficient. Since these latter two models predict steady-state heat fluxes which bracket that predicted from more realistic models, it is felt that their use in the transient analysis should give satisfactory results.

MATHEMATICAL MODELS

Two models are considered; the fluid velocity is modeled by a plug flow and by a linear velocity profile as shown in Fig. 1 and Fig. 2 respectively. It is assumed in both models that the fluid velocity is fully developed, axial conduction and viscous dissipation are negligible, the fluid properties are constant, the contact time is short so that the temperature variations are confined to a region close to the wall separating the two streams, and that there is no resistance to heat transfer in the wall. Under these conditions, the dimensionless equations governing the two streams are:

$$\left.\begin{aligned} \frac{\partial\theta_1}{\partial\tau} + \frac{\partial\theta_1}{\partial\xi} &= \frac{\partial^2\theta_1}{\partial\eta^2} \\ B\frac{\partial\theta_2}{\partial\tau} - \frac{\partial\theta_2}{\partial\xi} &= A\frac{\partial^2\theta_2}{\partial\eta^2} \end{aligned}\right\} \quad (2)$$

for plug flow, and

$$\left.\begin{aligned} \frac{\partial\theta_1}{\partial\tau} + \eta\frac{\partial\theta_1}{\partial\xi} &= \frac{\partial^2\theta_1}{\partial\eta^2} \\ B\frac{\partial\theta_2}{\partial\tau} + \eta\frac{\partial\theta_2}{\partial\xi} &= A\frac{\partial^2\theta_2}{\partial\eta^2} \end{aligned}\right\} \quad (3)$$

for the linear velocity profile.

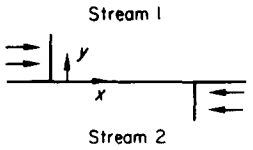

FIG. 1. Plug flow model.

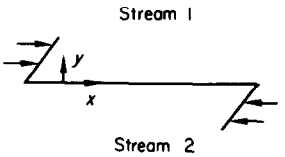

FIG. 2. Linear velocity profile model.

Steady state

For steady state, the transient terms are zero and the boundary conditions for both flow models are:

$$\begin{aligned} &\xi = 0, && \theta_1 = 0, \eta > 0 \\ &\xi = 1, && \theta_2 = 1, \eta < 0 \\ &\eta = \infty, && \theta_1 = 0 \\ &\eta = -\infty, && \theta_2 = 1 \end{aligned} \quad (4)$$

$$\eta = 0, \theta_1 = \theta_2 = \theta_w, k_1\frac{\partial\theta_1}{\partial\eta} = k_2\frac{\partial\theta_2}{\partial\eta}, \quad 0 < \xi < 1.$$

Taking the Laplace transform of equations (2) and (3) with respect to ξ and ξ' yields:

$$s\hat{\theta}_1 = \frac{d^2\hat{\theta}_1}{d\eta^2}, \qquad s'\hat{\theta}'_2 = A\frac{d^2\hat{\theta}'_2}{d\eta'^2} \quad (5)$$

for plug flow, and

$$s\eta\hat{\theta}_1 = \frac{d^2\hat{\theta}_1}{d\eta^2}, \qquad s'\eta'\hat{\theta}'_2 = A\frac{d^2\hat{\theta}'_2}{d\eta'^2} \quad (6)$$

for the linear velocity profile. The primed quantities are:

$$\begin{aligned} &\xi' = 1 - \xi \\ &\theta' = 1 - \theta \\ &\eta' = -\eta \\ &s' = \text{Laplace transform variable for } \xi'. \end{aligned} \quad (7)$$

The equations (5) or (6) are subject to the boundary conditions $\hat{\theta}_1(\infty) = \hat{\theta}'_2(\infty) = 0$. Neither the

temperature nor the heat flux is known at the surface between the two streams. However, let $\theta_w(\xi)$ (as yet unknown) be the surface temperature. The boundary conditions for (5) or (6) at the surface are then

$$\hat{\theta}_1(0) = \hat{\theta}_w \tag{8}$$

$$\hat{\theta}'_2(0) = \hat{\theta}'_w. \tag{9}$$

Solutions can then be found to (5) or (6) in terms of the transformed wall temperature. The inverse transforms are then taken yielding the temperature field in terms of $\theta_w(\xi)$. Thus the gradient of the temperature at the surface can be obtained. For the plug flow, there is

$$\left.\frac{\partial\theta_1}{\partial\eta}\right|_{\eta=0} = \frac{\theta_w(0^+)}{(\pi\xi)^{\frac{1}{2}}} + \frac{1}{(\pi)^{\frac{1}{2}}}\int_{0^+}^{\xi}\frac{1}{(\xi-\lambda)^{\frac{1}{2}}}\frac{\mathrm{d}\theta_w}{\mathrm{d}\lambda}\mathrm{d}\lambda \tag{10}$$

and

$$\frac{k_2}{k_1}\left.\frac{\partial\theta_2}{\partial\eta}\right|_{\eta=0} = \frac{1}{\beta}\left[\frac{1-\theta_w(1^-)}{\pi^{\frac{1}{2}}(1-\xi)^{\frac{1}{2}}} + \frac{1}{\pi^{\frac{1}{2}}}\int_{\xi}^{1^-}\times\frac{1}{(\lambda-\xi)^{\frac{1}{2}}}\frac{\mathrm{d}\theta_w}{\mathrm{d}\lambda}\mathrm{d}\lambda\right], \tag{11}$$

with similar equations for the linear velocity profile. The heat fluxes at the surface for the two streams are then equated for $0<\xi<1$, yielding

$$\frac{\theta_w(0^+)}{\xi^{\frac{1}{2}}} + \int_{0^+}^{\xi}\frac{1}{(\xi-\lambda)^{\frac{1}{2}}}\frac{\mathrm{d}\theta_w}{\mathrm{d}\lambda}\mathrm{d}\lambda = \frac{1}{\beta}\left[\frac{1-\theta_w(1^-)}{(1-\xi)^{\frac{1}{2}}} + \int_{\xi}^{1^-}\frac{1}{(\lambda-\xi)^{\frac{1}{2}}}\frac{\mathrm{d}\theta_w}{\mathrm{d}\lambda}\mathrm{d}\lambda\right] \tag{12}$$

for plug flow. In a similar manner there is for the linear velocity profile

$$\frac{\theta_w(0^+)}{\xi^{\frac{1}{2}}} + \int_{0^+}^{\xi}\frac{1}{(\xi-\lambda)^{\frac{1}{2}}}\frac{\mathrm{d}\theta_w}{\mathrm{d}\lambda}\mathrm{d}\lambda = \frac{1}{\gamma}\left[\frac{1-\theta_w(1^-)}{(1-\xi)^{\frac{1}{2}}} + \int_{\xi}^{1^-}\frac{1}{(\lambda-\xi)^{\frac{1}{2}}}\frac{\mathrm{d}\theta_w}{\mathrm{d}\lambda}\mathrm{d}\lambda\right]. \tag{13}$$

The interval $0<\xi<1$ is then divided into N points and $\mathrm{d}\theta_w/\mathrm{d}\lambda$ is approximated by a difference between consecutive points. Equations (12) and (13) yield N algebraic equations since the heat fluxes of the two streams must be equal at all N points. For example, equation (12) becomes:

$$\beta\frac{\theta_{w(n=1)}}{\xi_n^{\frac{1}{2}}} + \beta\sum_{j=1}^{n-1}\left[\frac{\theta_{w(j+1)}-\theta_{w(j)}}{\xi_{j+1}-\xi_j}\right]\int_{\xi_j}^{\xi_{j+1}}\times\frac{\mathrm{d}\lambda}{(\xi_n-\lambda)^{\frac{1}{2}}} = \frac{1-\theta_{w(n=N)}}{(1-\xi_n)^{\frac{1}{2}}} + \sum_{j=n}^{N-1}\times\left[\frac{\theta_{w(j+1)}-\theta_{w(j)}}{\xi_{j+1}-\xi_j}\right]\int_{\xi_j}^{\xi_{j+1}}\frac{\mathrm{d}\lambda}{(\lambda-\xi_n)^{\frac{1}{2}}}, \tag{14}$$

where $n = 1, 2, \ldots, N$.

There is a similar expression for equation (13). The resulting equations were solved on the IBM 7094 computer.

Convergence was checked by breaking the interval into 101 points and 50 points, where the 50 point approximation was formed by using the second, fourth, sixth, etc., points of the 100 point approximation. The spacing was unequal, being much closer together near the ends to account for rapid changes in the wall temperature. In the numerical calculations, for the 101 point case, $\xi_1 = 1{\cdot}5\times10^{-4}$. In comparing the 101 point case to the 50 point case, it was found that θ_w varied by less than one per cent over the range $0{\cdot}005 \leqslant \xi \leqslant 0{\cdot}995$.

No assumption was made on the surface temperatures at $\xi = 0$ and $\xi = 1$. However, the results of the computations showed that $\theta_w \to 0$ as $\xi \to 0$ and $\theta_w \to 1$ as $\xi \to 1$. This was checked by repeating the calculations assuming that $\theta_w(0) = 0$ and $\theta_w(1) = 1$; this had no effect on the results.

The local wall temperatures for the two models are compared in Fig. 3 for $\beta = \gamma = 1{\cdot}0$. It is noted that $\beta = \gamma = 1$ can represent the case in which the two streams are the same fluid at the same velocities. If β or γ is greater

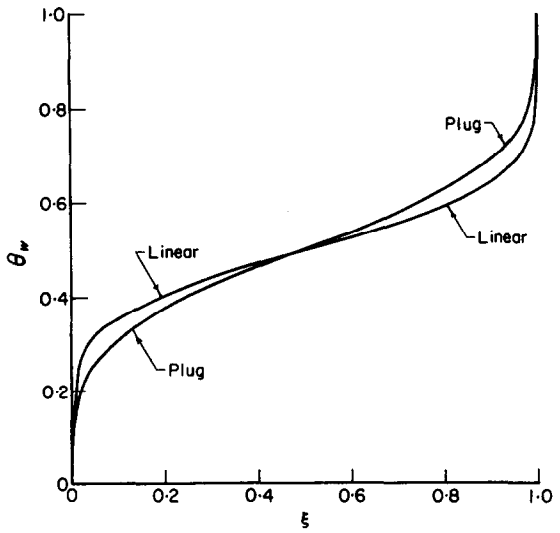

FIG. 3. Local wall temperature comparison, $\beta = 1$, $\gamma = 1$.

than one, stream one has a higher velocity, heat capacity or conductivity. The wall temperature near the entrance region increases or decreases less rapidly with distance in the case of plug flow since the model allows for greater convection near the wall.

The local wall heat flux for plug flow is obtained from (10). The local and average heat-transfer coefficients obtained were then compared to that calculated from equation (1); the individual coefficients h_1 and h_2 were obtained either by assuming a constant wall temperature or a constant wall heat flux. The average heat-transfer coefficients used for comparison are denoted by $\overline{U}_T$ and $\overline{U}_Q$ respectively. The ratios of the local overall heat-transfer coefficients for the two models to $\overline{U}_T$ are shown in Fig. 4 for $\beta = \gamma = 1$. The average overall coefficients for the two models are shown in Fig. 5 as functions of β and γ. Comparisons to

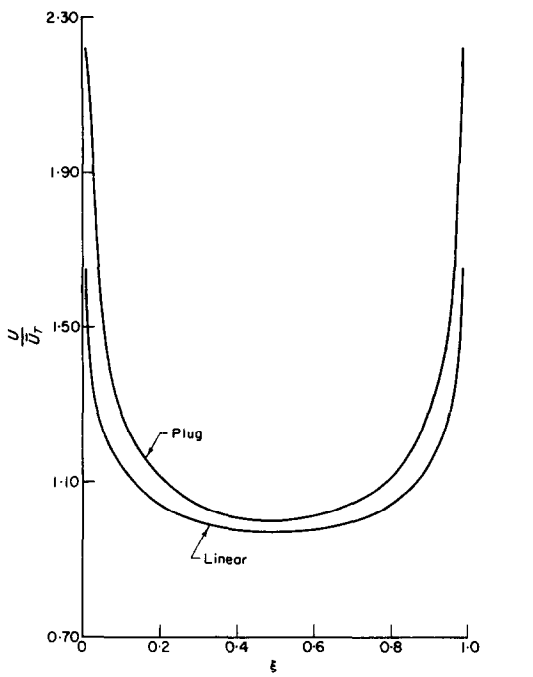

FIG. 4. Comparison of overall heat-transfer coefficients, $\beta = 1$, $\gamma = 1$.

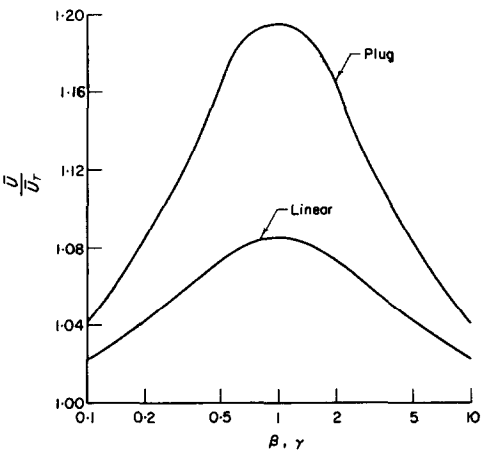

FIG. 5. Average overall heat-transfer coefficients normalized with respect to $\overline{U}_T$.

$\overline{U}_Q$ were made but are not shown. The heat-transfer coefficients for both models are always higher than $\overline{U}_T$ and lower than $\overline{U}_Q$. The coefficient predicted from the linear velocity profile shows less deviation from $\overline{U}_T$ and $\overline{U}_Q$ than that predicted from the plug flow model for all values of β and γ. The plug flow model has been treated previously by King [9] by an iterative scheme. The results were duplicated in order to check the method described above. Complete agreement was obtained.

TRANSIENT BEHAVIOR

Mathematical approach

Consideration is now given to the transient behavior. The system is initially at some steady state which is described and analyzed above. At time $\tau = 0$ a change is made in the velocity of stream one; the velocity of stream two is not changed. The inlet temperatures of the two streams also are unchanged. Since the relative velocities have been altered, the temperatures and the heat flux at the surface will be perturbed and will decay to some new steady state. For ease of analysis, only plug flow velocity profiles are considered. The velocity of stream one changes instantaneously from u_{10} to u_1 causing a change in temperature from θ_{j0} to θ_j, $j = 1$ or 2. The substitution $\theta_j = \theta_{j0} + \theta_{jt}$ is made where θ_{jt} is the perturbation away from the initial steady-state temperature. The energy equation (2) then becomes

$$\frac{\partial\theta_{1t}}{\partial\tau} + \frac{\partial\theta_{10}}{\partial\xi} + \frac{\partial\theta_{1t}}{\partial\xi} = \frac{\partial^2\theta_{10}}{\partial\eta^2} + \frac{\partial^2\theta_{1t}}{\partial\eta^2} \quad (15a)$$

$$B\frac{\partial\theta_{2t}}{\partial\tau} - \frac{\partial\theta_{20}}{\partial\xi} - \frac{\partial\theta_{2t}}{\partial\xi} = A\left[\frac{\partial^2\theta_{20}}{\partial\eta^2} + \frac{\partial^2\theta_{2t}}{\partial\eta^2}\right]. \quad (15b)$$

The independent variable η and the parameter A in (15a) and (15b) are defined in terms of u_1, where u_1 is the velocity to which stream one is perturbed. Before the perturbation of the velocity of stream one, the system was at some initial steady state. The equations governing this initial steady state are

$$\frac{u_{10}}{u_1}\frac{\partial\theta_{10}}{\partial\xi} = \frac{\partial^2\theta_{10}}{\partial\eta^2} \quad (15c)$$

$$-\frac{\partial\theta_{20}}{\partial\xi} = A\frac{\partial^2\theta_{20}}{\partial\eta^2}. \quad (15d)$$

The factor u_1/u_{10} arises since the velocity of stream one at the initial steady state was u_{10} whereas η and A are now defined in terms of u_1. Subtracting (15c) and (15d) from (15a) and (15b) respectively then yields

$$\frac{\partial\theta_{1t}}{\partial\tau} + \frac{\partial\theta_{1t}}{\partial\xi} = \frac{\partial^2\theta_{1t}}{\partial\eta^2} + \left(\frac{u_{10}}{u_1} - 1\right)\frac{\partial\theta_{10}}{\partial\xi}, \quad (16a)$$

$$B\frac{\partial\theta_{2t}}{\partial\tau} + \frac{\partial\theta_{2t}}{\partial\xi'} = A\frac{\partial^2\theta_{2t}}{\partial\eta^2}, \quad \text{where } \xi' = 1 - \xi. \quad (16b)$$

The boundary and initial conditions are:

$$\begin{aligned}
&\tau \leqslant 0, \quad \theta_{1t} = \theta_{2t} = 0\\
&\xi = 0, \quad \theta_{1t} = 0, \quad \eta > 0\\
&\xi' = 0, \quad \theta_{2t} = 0, \quad \eta < 0\\
&\eta = \infty, \quad \theta_{1t} = 0; \quad \eta = -\infty, \quad \theta_{2t} = 0\\
&\eta = 0, \quad \theta_{1t} = \theta_{2t} = \theta_{wt}; \quad k_1\frac{\partial\theta_{1t}}{\partial\eta} = k_2\frac{\partial\theta_{2t}}{\partial\eta}, \quad 0 < \xi < 1.
\end{aligned} \quad (17)$$

The Laplace transforms of equations (16a) and (16b) with respect to τ and ξ and τ and ξ' respectively are

$$p\hat{\bar{\theta}}_{1t} + s\hat{\bar{\theta}}_{1t} = \frac{d^2\hat{\bar{\theta}}_{1t}}{d\eta^2} + \left(\frac{u_{10}}{u_1} - 1\right)\frac{s}{p}\hat{\theta}_{10}, \quad (18a)$$

and

$$Bp\hat{\bar{\theta}}_{2t} + s'\hat{\bar{\theta}}_{2t} = A\frac{d^2\hat{\bar{\theta}}_{2t}}{d\eta^2} \quad (18b)$$

where

$$\hat{\theta}_{10} = \hat{\theta}_{w0}\exp\left[-\left(\frac{u_{10}}{u_1}s\right)^{\frac{1}{2}}\eta\right].$$

The transform variables for τ, ξ, and ξ' are p, s, and s' respectively. Equations (18a) and (18b) can now be solved with the aid of the boundary conditions (17) to give the wall heat flux in terms of the yet unknown wall temperature $\hat{\bar{\theta}}_{wt}$:

$$-\left.\frac{d\hat{\bar{\theta}}_{1t}}{d\eta}\right|_{\eta=0} = \hat{\bar{\theta}}_{wt}(s + p)^{\frac{1}{2}}$$

$$+\frac{s\left(1-\frac{u_{10}}{u_1}\right)\left[(s+p)^{\frac{1}{2}}-\left(\frac{u_{10}}{u_1}s\right)^{\frac{1}{2}}\right]\hat{\theta}_{w0}}{p\left[p+s\left(1-\frac{u_{10}}{u_1}\right)\right]} \quad (19a)$$

$$-\left.\frac{\mathrm{d}\hat{\theta}'_{2t}}{\mathrm{d}\eta}\right|_{\eta=0}=-\hat{\theta}'_{wt}\left(\frac{Bp+s'}{A}\right)^{\frac{1}{2}}, \quad (19b)$$

where $\theta'\ (\tau,\xi')=\theta(\tau,1-\xi')$.

The inverse of equations (19a) and (19b) with respect to p are:

$$-\left.\frac{\partial\hat{\theta}_{1t}}{\partial\eta}\right|_{\eta=0}=\int_0^\tau\left[\frac{1}{\pi^{\frac{1}{2}}(\tau-\zeta)^{\frac{1}{2}}}\exp\left[-s(\tau-\zeta)\right]+s^{\frac{1}{2}}\operatorname{erf}\left[s^{\frac{1}{2}}(\tau-\zeta)^{\frac{1}{2}}\right]\right]\frac{\partial\hat{\theta}_{wt}}{\partial\zeta}\mathrm{d}\zeta$$
$$+\frac{(1-u_{10}/u_1)}{\pi^{\frac{1}{2}}}\int_0^\tau\frac{s\hat{\theta}_{w0}}{\zeta^{\frac{1}{2}}}\left\{\exp(-s\zeta)\times\left[1-(\pi\zeta s u_{10}/u_1)^{\frac{1}{2}}\exp(s\zeta u_{10}/u_1)\times\operatorname{erfc}(\zeta s u_{10}/u_1)^{\frac{1}{2}}\right]\right\}\mathrm{d}\zeta, \quad (20a)$$

$$-\left.\frac{\partial\hat{\theta}'_{2t}}{\partial\eta}\right|_{\eta=0}=-\left(\frac{B}{A}\right)^{\frac{1}{2}}\times\int_0^\tau\left\{\frac{1}{\pi^{\frac{1}{2}}(\tau-\zeta)^{\frac{1}{2}}}\exp\left[\frac{-s'(\tau-\zeta)}{B}\right]+\left(\frac{S'}{B}\right)^{\frac{1}{2}}\operatorname{erf}\left[\left(\frac{S'}{B}\right)^{\frac{1}{2}}(\tau-\zeta)^{\frac{1}{2}}\right]\right\}\frac{\partial\hat{\theta}'_w}{\partial\zeta}\partial\zeta. \quad (20b)$$

The inverses of equations (20a) and (20b) are:

$$-\left.\frac{\partial\theta_{1t}}{\partial\eta}\right|_{\eta=0}=\frac{\left(1-\frac{u_{10}}{u_1}\right)\left(\frac{u_{10}}{u_1}\right)^{\frac{1}{2}}}{2\pi^{\frac{1}{2}}}f(\tau,\xi)+\frac{1}{\pi^{\frac{1}{2}}}\int_0^\tau\int_0^\xi K_1(\tau-\zeta,\xi-\lambda)\frac{\partial^2\theta_{wt}}{\partial\zeta\partial\lambda}\mathrm{d}\lambda\mathrm{d}\zeta, \quad (21a)$$

$$-\frac{k_2}{k_1}\left.\frac{\partial\theta'_{2t}}{\partial\eta}\right|_{\eta=0}=-\frac{1}{\beta\pi^{\frac{1}{2}}}\int_0^\tau\int_0^{\xi'}K_2(\tau-\zeta,\xi'-\lambda')\times\frac{\partial^2\theta'_{wt}}{\partial\zeta\partial\lambda'}\mathrm{d}\lambda'\,\mathrm{d}\zeta, \quad (21b)$$

where:

$$f(\tau,\xi)=\begin{cases}\displaystyle\int_0^\tau\int_0^{\xi-\zeta}\frac{1}{\left[(\xi-\lambda-\zeta)+\frac{u_{10}}{u_1}\zeta\right]^{\frac{1}{2}}}\frac{\mathrm{d}\theta_{w0}}{\mathrm{d}\lambda}\mathrm{d}\lambda\mathrm{d}\zeta, & \tau<\xi\\ \displaystyle\int_0^\xi\int_0^{\xi-\zeta}\frac{1}{\left[(\xi-\lambda-\zeta)+\frac{u_{10}}{u_1}\zeta\right]^{\frac{1}{2}}}\frac{\mathrm{d}\theta_{w0}}{\mathrm{d}\lambda}\mathrm{d}\lambda\mathrm{d}\zeta, & \tau\geqslant\xi\end{cases} \quad (22a)$$

$$K,(\tau-\zeta,\xi-\lambda)=\begin{cases}\dfrac{1}{(\tau-\zeta)^{\frac{1}{2}}}, & 0\leqslant\lambda<\xi-\tau+\zeta\\ \dfrac{1}{(\xi-\lambda)^{\frac{1}{2}}}, & \xi-\tau+\zeta\leqslant\lambda<\xi\\ \dfrac{1}{(\xi-\lambda)^{\frac{1}{2}}}, & 0\leqslant\lambda\leqslant\xi,\quad\xi\leqslant\tau-\zeta,\end{cases}\quad \xi>\tau-\zeta \quad (22b)$$

$$K_2(\tau-\zeta,\xi'-\lambda')=\begin{cases}\dfrac{B^{\frac{1}{2}}}{(\tau-\zeta)^{\frac{1}{2}}}, & 0\leqslant\lambda'<\xi'-\left(\dfrac{\tau-\zeta}{B}\right)\\[2ex] \dfrac{1}{(\xi'-\lambda')^{\frac{1}{2}}}, & \xi'-\left(\dfrac{\tau-\zeta}{B}\right)\leqslant\lambda'\leqslant\xi'\\[2ex] \dfrac{1}{(\xi'-\lambda')^{\frac{1}{2}}} & 0\leqslant\lambda'\leqslant\xi',\ \xi'\leqslant\dfrac{\tau-\zeta}{B}.\end{cases}\quad \xi'>\frac{\tau-\zeta}{B} \tag{22c}$$

It has been assumed in the above that $\theta_{wt}(0)=\theta_{wt}(1)=0$. The steady-state numerical results indicate that this is true.

The wall temperature, θ_{wt}, is approximated by the series

$$\theta_{wt}\cong\sum_{k=1}^{m}W_k(\xi)\,\psi_k(\tau) \tag{23}$$

where the $W_k(\xi)$ are chosen to satisfy the boundary conditions. There are now m unknowns, namely $\psi_k(\tau)$, $k=1, 2, \ldots m$. To generate m equations, equations (21a) and (21b) are multiplied by the weighting function ξ^l, $l=0, 1, \ldots, m-1$, and integrated over ξ from 0 to 1. The resulting integrals from the right hand side of (21a) and (21b) are equated for each value of l. The resulting system of equations is:

$$\begin{aligned}-\left(1-\frac{u_{10}}{u_1}\right)\left(\frac{u_{10}}{u_1}\right)^{\frac{1}{2}}\int_0^1\xi^l f(\tau,\xi)\,\mathrm{d}\xi\\ =2\sum_k\left\{\int_0^\tau\left[\int_0^1\int_0^\xi\xi^l K_1\frac{\mathrm{d}W_k}{\mathrm{d}\lambda}\mathrm{d}\lambda\mathrm{d}\xi,\right.\right.\\ l=0,1,\ldots,m-1.\\ \left.\left.+\frac{1}{\beta}\int_0^1\int_0^{\xi'}(1-\xi')^l K_2\frac{\mathrm{d}W'_k}{\mathrm{d}\lambda'}\mathrm{d}\lambda'\mathrm{d}\xi'\right]\right.\\ \left.\times\frac{\mathrm{d}\psi_k}{\mathrm{d}\zeta}\mathrm{d}\zeta\right\}\end{aligned} \tag{24}$$

where $W'(\xi')=W(1-\xi')$.

To solve equation (24), the interval $(0,\tau)$ is broken into a number of points and $\mathrm{d}\psi_k/\mathrm{d}\zeta$ is approximated by a difference. The solution then requires solving an m by m matrix at each time step. The average flux is given by:

$$\overline{Q}_w(\tau)=\overline{Q}_{wo}+\frac{1}{\beta\pi^{\frac{1}{2}}}\times\sum_k\int_0^\tau\left\{\int_0^1\int_0^{\xi'}K_2\frac{\mathrm{d}W'_k}{\mathrm{d}\lambda'}\mathrm{d}\lambda'\mathrm{d}\xi'\right\}\frac{\mathrm{d}\psi_k}{\mathrm{d}\zeta}\mathrm{d}\zeta, \tag{25}$$

where $\overline{Q}_{wo}$ is obtained from the steady-state solution. Numerical solutions to (24) were carried out with one, two and three term expansions. The expansion functions chosen were $W_1(\xi)=\xi(1-\xi)$, $W_2(\xi)=\xi^4(1-\xi)$, and $W_3(\xi)=\xi(1-\xi)^4$. The fourth powers were used since the steady-state results indicate that the surface temperature depends strongly on ξ near $\xi=0$ and $\xi=1$. Since the series (23) had to be truncated after only three terms because of the complexity of the equations, the results are approximate. However, a comparison of the results obtained from (25) using one, two and three terms indicates that the solution converges toward some result [14]. This comparison is discussed below. There is also a second indication that these approximate solutions are reasonable; the average flux reached at large time was independently calculated using the methods discussed above for the steady state. The final average flux reached by the transient solution was then compared to the accurate steady-state result. Agreement was good as noted below.

A comparison in the steady-state case is made in Figs. 4 and 5 between the calculated heat flux and the heat flux found using an overall heat-transfer coefficient from equation (1) in which the individual coefficients are those for a constant temperature wall. It is desired to make a similar comparison for the transient case. For this, the transient equations are solved assuming that the unknown wall temperature is a function of time but not of position. Equations (19a) and (19b) are used with the substitution $\hat{\theta}_{wt} = \hat{\theta}_{wt}(p/s$ and $\hat{\theta}'_{wt} = \hat{\theta}_{wt}(P)/S'$ being made. This procedure is analogous to the determination of $\overline{U}_T$ used in the steady-state solutions. The inverses are taken and the average wall flux of the two streams equated. The values of θ_{wo} are taken from the steady-state solutions obtained using $\overline{U}_T$. The resulting equations are

$$F_1(\tau) = F_2(\tau)$$

$$F_1 = -2\left(\frac{1}{1+\beta_0}\right)\left\{\tau^{\frac{1}{2}} + \left(\frac{u_{10}}{u_1}\right)^{\frac{1}{2}} \times \left[(1-\tau) + \frac{u_{10}}{u_1}\tau\right]^{\frac{1}{2}} - \frac{u_{10}}{u_1}\tau^{\frac{1}{2}} - \left(\frac{u_{10}}{u_1}\right)^{\frac{1}{2}}\right\}$$

$$= -\int_0^\tau \left[(\tau-\zeta)^{-\frac{1}{2}} + (\tau-\zeta)^{\frac{1}{2}}\right]\frac{d\theta_{wt}}{d\zeta}\,d\zeta, \quad \tau < 1$$

$$F_2 = +\frac{1}{\beta}\int_0^\tau \left[\left(\frac{\tau-\zeta}{B}\right)^{-\frac{1}{2}} + \left(\frac{\tau-\zeta}{B}\right)^{\frac{1}{2}}\right]\frac{d\theta_{wt}}{d\zeta}\,d\zeta,$$

$$F_1 = -2\left(\frac{1}{1+\beta_0}\right)\left[1 - \left(\frac{u_{10}}{u_1}\right)^{\frac{1}{2}}\right] - 2\theta_{wt}(\tau-1) - \int_{\tau-1}^\tau \left[(\tau-\zeta)^{-\frac{1}{2}} + (\tau-\zeta)^{\frac{1}{2}}\right]\frac{d\theta_{wt}}{d\zeta}\,d\theta, \quad \tau > 1$$

$$F_2 = +\frac{2\theta_{wt}(\tau-B)}{\beta} + \int_{\tau-B}^\tau \left[\left(\frac{\tau-\zeta}{B}\right)^{-\frac{1}{2}} + \left(\frac{\tau-\zeta}{B}\right)^{\frac{1}{2}}\right]\frac{d\theta_{wt}}{d\zeta}\,d\zeta, \quad \tau > B. \tag{26}$$

The average wall heat flux is:

$$\overline{Q}_{wt}(\tau) = -\frac{1}{\beta\pi^{\frac{1}{2}}} \times \int_0^\tau \left[\left(\frac{\tau-\zeta}{B}\right)^{-\frac{1}{2}} + \left(\frac{\tau-\zeta}{B}\right)^{\frac{1}{2}}\right]\frac{d\theta_{wt}}{d\zeta}\,d\zeta, \quad \tau < B,$$

$$= -2\frac{\theta_{wt}(\tau-B)}{\beta\pi^{\frac{1}{2}}} - \frac{1}{\beta\pi^{\frac{1}{2}}} \times \int_{\tau-B}^\tau \left[\left(\frac{\tau-\zeta}{B}\right)^{-\frac{1}{2}} + \left(\frac{\tau-\zeta}{B}\right)^{\frac{1}{2}}\right]\frac{d\theta_{wt}}{d\zeta}\,d\zeta, \quad \tau \geqslant B. \tag{27}$$

The total average wall heat flux is $\overline{Q}_w(\tau) = \overline{Q}_{w0} + \overline{Q}_{wt}$, where

$$\overline{Q}_{w0} = \frac{2}{\pi^{\frac{1}{2}}}\left(\frac{1}{1+\beta_0}\right). \tag{28}$$

To solve equation (26), $d\theta_{wt}/d\zeta$ is approximated by a difference. Solutions found from (24) and (25) were then compared to those found from the simpler (26) and (28). It is noted that the solution using (26) is equivalent to using $\overline{U}_T$ in the steady-state comparison.

DISCUSSION

The system is governed by the three parameters β_0, β, and B, since $u_{10}/u_1 = (\beta_0/\beta)^2$. The only difference between β_0 and β is that for β_0, u_{10} is used and for β, the new velocity u_1 is used. B is the ratio of the new stream one velocity to the unchanged velocity of stream two.

Some results for the case $\beta_0 = 1{\cdot}0$, $\beta = 1{\cdot}1$, and $B = 1{\cdot}21$ are shown in Fig. 6. This would correspond to stream one and stream two consisting of the same fluid initially at the same velocities. At time $\tau = 0$, the velocity of stream one is increased by 21 per cent. The average heat flux between the two streams as a function of time is shown. Results are presented for one, two and three term expansions. The two and three term expansions yield identical results for the average wall heat flux to the accuracy of the

graph. The results for all three expansions rise to maxima before leveling out to a new steady state. It is noted that the steady state which must be approached is known *a priori* from the steady-state numerical results presented above, and is denoted by the dotted line labeled "Steady state". The values to which the one, two and three term expansions converge are denoted by dotted lines labeled "∞". The average wall heat flux given by the two and three term expansions proceed to the correct steady state; that predicated by the one term expansion is about 2 per cent high. The fact that the two and three term expansions go to the correct steady state gives further confidence in the method of solution.

It is noted that the average wall heat flux can be found in the limit as $\tau \to \infty$ without solving the transient equations as functions of τ; any number of terms in the expansion can be used. In this way, the limit as $\tau \to \infty$ predicted by the approximate transient equations can be compared to the correct final steady-state results before the numerical solution for all τ is obtained; this gives an *a priori* indication of the error introduced by truncating the series expansion at any length. To do this, the left-hand side of equation (24) is calculated numerically for $\tau \to \infty$. From equation (22a) it is seen that the left-hand side of equation (24) is constant for τ greater than one. The integrals on the right-hand side of equation (24) can also be calculated for $\tau \to \infty$ by employing equations (22b) and (22c) and assuming that $d\psi_k/d\tau$, $k = 1, 2, \ldots$, approaches zero as $\tau \to \infty$. Therefore, the values of ψ_k as $\tau \to \infty$ can be found from the solution of a set of linear algebraic equations. Thus from equation (25) the average wall heat flux can be obtained for $\tau \to \infty$. Details can be found in [14].

The one term expansion yields results which are somewhat in error as shown by Fig. 6. The same type of agreement was obtained in comparisons of the one, two, and three term expansions in other cases which are not shown here. The results using a one term expansion are sufficiently accurate, however, to point out qualitative trends in the transient behavior of the countercurrent flows under consideration. The use of a one term expansion in an extensive study is necessitated by the amount of computer time which is required for the longer expansions.

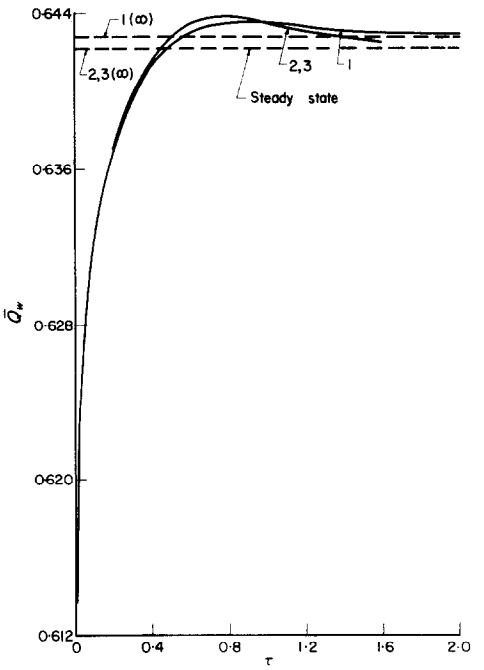

FIG. 6. Average wall heat flux, 1 = one term, 2 = two term, 3 = three term, $\beta_0 = 1{\cdot}0$, $\beta = 1{\cdot}1$, $B = 1{\cdot}21$.

The local wall temperature did not approximate the solution nearly as well as the average flux. However, this is to be expected with an approach of this type.

Figure 7 shows the effect of perturbing from different initial conditions to the same final condition. The fluids are taken to be the same in both streams. It is seen that a longer time is required to reach steady state if the initial conditions are further away from the final steady state. The time at which the maxima occur seems to be independent of the initial steady state.

Figures 6 and 7 show overshoots in the average wall flux. It is not to be inferred that overshoots

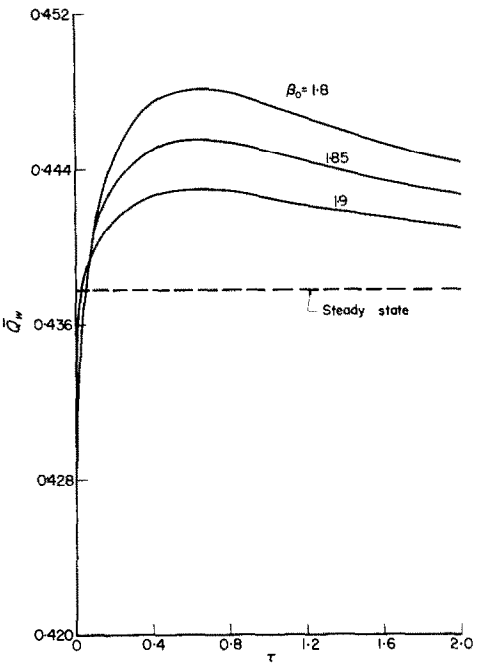

FIG. 7. Average wall heat flux, one term, $\beta = 2{\cdot}0$, $B = 4{\cdot}0$.

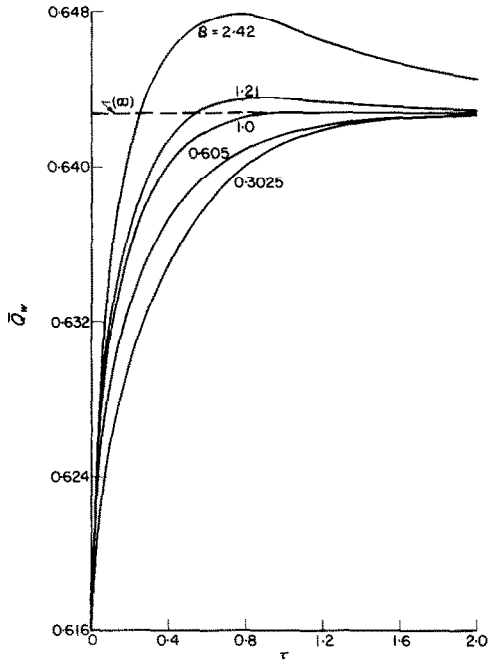

FIG. 8. Average wall heat flux, one term, with varying B, $\beta_0 = 1{\cdot}0$, $\beta = 1{\cdot}1$.

always occur. It was found that overshoots in the magnitude of the flux only occur when B is greater than one, i.e. when the final velocity of stream one is greater than that of stream two. If the velocity of stream one is decreased but is still greater than stream two, undershoots will occur.

Figure 8 shows the variation of the average wall flux for different values of B for the same β_0 and β. It is noted that a longer time is required to reach the new steady state as B increases from one, and that when B equals one the average flux reaches its new steady-state value at $\tau = 1$. For B less than one, the flux grows more slowly at small time but does not require a longer time to reach its final steady state.

To explain the overshoots physically, assume that stream one is the cold fluid, that the velocity of stream one is increased, and that B is greater than one. Reference is made to Fig. 9.

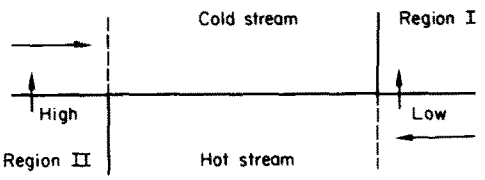

FIG. 9. Transient plug flow model.

Region I contains fluid of stream one present before the velocity change in stream one. Region II contains fluid of stream two present before the velocity change. In region I, the fluid of stream one will be warmer than that present at the final steady state, since it was initially moving more slowly, and therefore, its temperature near the wall will be closer to that of stream two. The flux in region I relative to the final steady state is therefore lower. In region II, the fluid of stream two near the wall will be warmer than that which will be there at the final steady state. This is true since stream two was initially in contact with a slower moving fluid. Therefore, there will be a higher flux in region II relative to that at the final steady state. Thus, if the new velocity of stream one is faster than stream

two, the effect of the high heat flux in region II can dominate over the low heat flux in region I and the possibility of an overshoot in the average wall heat flux arises. A similar argument can be made for the case when the velocity of stream one is decreased but is still greater than stream two. Although this argument does not insure the existance of overshoots and undershoots, it does show the possibility that they can occur

All maxima and minima occur before both streams have made one pass, i.e. τ less than B. The magnitude of the overshoots increases with increasing values of B. All major changes in the average flux occur before both streams make one pass and therefore this can be used to estimate the duration of the transient behavior.

It is also of interest to compare the above results with the transient heat flux which is predicted if the wall temperature is assumed to be independent of position but still a function of time. This comparison between methods of predicting the transient behavior is analogous to the comparison shown in Figs. 4 and 5 for the steady state. The heat flux predicted from a solution of equation (26) and (27) is shown in Fig. 10 for three initial conditions all proceeding to the same final steady state. This is to be compared to Fig. 7 which gives the results for the same problem using a one term expansion. It is noted that the fluxes in Figs. 7 and 10 do not proceed to the same final steady state. This is to be expected since the steady-state heat flux calculated assuming a constant temperature wall does not agree with the results using a variable temperature wall as shown in Figs. 4 and 5. The maxima are somewhat less pronounced in Fig. 10 than in Fig. 7; they occur roughly at the same time. The time required to reach steady state is also about the same. It is seen then that if for mathematical simplicity it is desired to model a transient countercurrent heat exchanger using equations (26) and (27) which assume a wall temperature independent of position or, equivalently by using an overall heat-transfer coefficient calculated from equation (1), that reasonable results would be obtained by multiplying the results by the appropriate factor taken from Fig. 5.

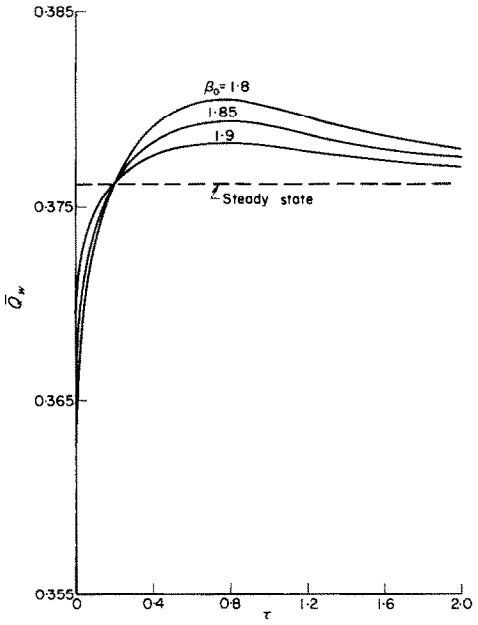

FIG. 10. Average wall heat flux, simplified model, $\beta = 2{\cdot}0$, $B = 4{\cdot}0$.

REFERENCES

1. R. J. NUNGE and W. N. GILL, Analysis of heat or mass transfer in some countercurrent flows, *Int. J. Heat Mass Transfer* **8**, 873 (1965).
2. R. J. NUNGE and W. N. GILL, An analytical study of laminar counterflow double-pipe heat exchangers, *A.I.Ch.E. Jl* **12**, 279 (1966).
3. R. P. STEIN, Liquid metal heat transfer, *Adv. Heat Transf.* **3**, 101 (1966).
4. R. P. STEIN, Mathematical and practical aspects of heat transfer in double pipe heat exchangers, in *Proceedings of the Third International Heat Transfer Conference*. Am. Inst. Chem. Engrs, New York (1966).
5. R. P. STEIN, Computational procedures for recent analyses of counterflow heat exchangers, *A.I.Ch.E. Jl* **12**, 1217 (1966).
6. J. A. BLANCO and W. N. GILL, Analysis of multistream turbulent forced convection systems, *Chem. Engng Prog. Symp. Ser.* 77 **63**, 66 (1967).
7. R. J. NUNGE, E. W. PORTA and W. N. GILL, Axial conduction in the fluid streams of multistream heat exchangers, *Chem. Engng Prog. Symp. Ser.* 77, **63**, 80 (1967).
8. E. N. LIGHTFOOT, Countercurrent heat or mass transfer between a turbulent and a laminar stream, *A.I.Ch.E. Jl* **8**, 416 (1962).

9. C. JUDSON KING, Mass transfer during short surface exposures in countercurrent flow, *I/EC Fundamentals* **4**, 125 (1965).
10. R. P. STEIN, The Graetz problem in co-current flow double pipe heat exchangers, presented at the Seventh National Heat Transfer Conference, A.I.Ch.E.–A.S.M.E., Cleveland (August 1964).
11. R. P. STEIN, Heat transfer coefficients in liquid metal co-current flow double pipe heat exchangers, presented at the Seventh National Heat Transfer Conference, A.I.Ch.E. A.S.M.E., Cleveland (August 1964).
12. P. S. LARSON and W-J. YANG, Frequency responses of multipass shell-and-tube type heat exchangers to timewise-variant flow perturbations, presented at the Seventh National Heat Transfer Conference, A.I.Ch.E.–A.S.M.E., Cleveland (August 1964).
13. M. MASUBUCHI, Dynamic response and control of multipass heat exchangers, *J. Bas. Engng* **82**, 51–65 (1960).
14. P. F. TOMLAN, Steady state and transient behavior of countercurrent heat exchangers with short contact time, M.S. Thesis, University of Illinois, Urbana (1967).

Résumé—Des solutions numériques sont obtenues pour le régime permanent et le comportement transitoire dans des échangeurs de chaleur à contre courant. En régime permanent, deux profils de vitesse simplifiés sont employés: écoulement en bloc et profil linéaire de vitesse. Les résultats sont comparés à la solutions classique employant l'addition de résistances, où l'on suppose que, soit la température pariétale, soit le flux de chaleur pariétal est constant.

Le problème transitoire résultant d'un changement de débit dans l'un des écoulements est résolu en supposant l'écoulement en bloc et une approximation en série pour la température pariétale. Ceci est comparé à un modèle simplifié employant une température pariétale moyenne indépendante de la position, mais variant avec le temps. On trouve que des dépassements dans le flux pariétal moyen se produisent dans les deux modèles lorsque le rapport de la vitesse de l'écoulement perturbé à la vitesse de l'autre écoulement est supérieur à l'unité.

Zusammenfassung—Für das stationäre und instationäre Verhalten von Gegenstrom-Wärmeübertragern mit kurzer Kontaktzeit werden numerische Lösungen angegeben. Bei der stationären Lösung werden zwei vereinfachte Geschwindigkeitsprofile verwendet: Kolbenströmung und ein lineares Geschwindigkeitsprofil. Die Ergebnisse werden mit der klassischen Lösung verglichen, bei der von einer Addition von Widerständen Gebrach gemacht wird, wobei entweder die Wantemperatur oder die Wärmestromdichte an der Wand als konstant vorausgesetz wird.

Das aus der Änderung einer der Mengenströme resultierende instationäre Problem lässt sich lösen, indem Kolbenströmung und eine Reiheapproximation für die Wandtemperatur angenommen wird.

Dieses Ergebnis wird mit einem vereinfachten Modell verglichen, bei dem eine zeitlich veränderliche aber örtlich konstant Wandtemperatur vorgegeben wird.

Es wurde ein Überschwingen der mittleren Wärmestromdichte an der Wand bei beiden Modellen festgestellt, sobald das Geschwindigkeitsverhältnis von gestörtem zu ungestörtem Strom den Wert eins übertraf.

Аннотация—Получены численные решения для стационарного и нестационарного режимов в противоточных теплообменниках с коротким периодом контакта. При решении для стационарного режима использовались два упрощенные профиля скорости: поршневое течение и линейный профиль скорости. Результаты сравнивались с классическим решением суммирования сопротивлений, в котором либо температура стенки, либо тепловой поток на ней принимаются постоянными.

Основываясь на допущении о поршневом течении и используя аппроксимацию для температуры стенки, получено решение задачи для переходного режима, возникающего при изменении расхода жидкости в одном из потоков.

Результаты сравниваются с упрощенной моделью, где используется средняя температура стенки, изменяющаяся во времени, но не зависящая от положения. Обнаружены резкие скачки среднего теплового потока на стенке в обеих моделях, когда отношение скорости изменяемого потока к скорости другого потока больше единицы.